Effect of Nano-TiO₂ on MP-25 Resin

Bin Xiang,[1] Zhang Shengtao,[1] Huang Wenzhang,[2] Hou Baorong[3]

[1]College of Chemistry and Chemical Engineering, Chongqing University, Chongqing 400044, China
[2]Chongqing University of Science and Technology, Chongqing 400012, China
[3]Institute of Oceanology, Chinese Academy of Sciences, Qingdao, 260071, China

ABSTRACT: MP-25 resin is a chlorine-containing polymer widely used in coatings. The effects of two types of nano-TiO₂ (P-25 and RM301 LP) on MP-25 were studied with saline immersion, UV irradiation, and electrochemical impedance spectroscopy. UV irradiation was evaluated in terms of gloss change and X-ray photoelectron spectroscopy (XPS). The results indicate that, compared to pigment R-930 TiO₂, P-25 reduced the immersion resistance and accelerated UV aging of the MP-25 coating, whereas RM301 LP showed the opposite effects. XPS analysis showed that MP-25 resin degraded under UV irradiation via dechlorination and C—C bond breakage, similarly to poly(vinyl chloride), but RM301 LP could inhibit the aging of MP-25 to a certain extent. A skin effect of oxygen and chlorine was identified in MP-25 resin by XPS. RM301 LP could improve the impedance of the MP-25 coating because of its excellent fill capacity. Hence, rutile nano-TiO₂ RM301 LP represents an excellent additive for MP-25 resin. © 2007 Wiley Periodicals, Inc. J Appl Polym Sci 107: 1598–1603, 2008

Key words: degradation; dyes/pigments; electrochemistry; nanotechnology

INTRODUCTION

MP serial chlorinated resins are copolymers of vinyl chloride and vinyl isobutyl ether. They can be used as the base resin for air-drying or other physical-drying paints. At present, only BASF Corp. (Ludwigshafen, Germany) and a Chinese plant can produce these items. The BASF products are the LaroFlex resin series, which include MP-15, MP-25, MP-35, MP-45, and MP-60. LaroFlex MP is a universal range of binders with a wide choice of viscosities. Because of its microstructure, LaroFlex MP has outstanding properties. These include the absence of carbon tetrachloride, excellent solubility, compatibility with many other raw materials, ease of processing, internal plasticization, good weather resistance even in aggressive atmospheres, excellent adhesion on critical surfaces, and aromatic-free formulas for the nonhydrolyzability of the monomers vinyl chloride and vinyl isobutyl ether.

MP chlorinated resins, especially MP-25 and MP-35, can be used in chemical-resistant coatings for steel structures, anticorrosion coatings, light metal coatings, deck paints, marine paints, container paints, engineering paints for mechanical equipment and automobiles, and flame-retardant paints for buildings. They are also used in the printing-ink industry and can be used as modifiers in rubber and plastic products. Moreover, MP resins offer advantages to both manufacturers and users of coatings because of their broad choice of solvents, particularly budget-priced blends of aromatic and aliphatic hydrocarbons, and good pigment-binding capacity, even at high contents of solids.

Chlorinated rubber has long been widely used as an anticorrosion coating because of its excellent qualities. However, the production process for chlorinated rubber required the use of carbon tetrachloride, an environmentally hazardous material, as a solvent in the past. International convention has banned the production of chlorinated rubbers using carbon tetrachloride since 2004. This led to a requirement for environmentally friendly products to substitute for traditional chlorinated rubber, which prompted the development of MP resins by BASF. Until now, MP-25 has been widely used in the coating industry, especially for heavy-duty anticorrosion coatings.[1]

Chlorinated polymers are prone to UV degradation. MP-25 resin has a chloromethylene group in each comonomer unit; as a result, this material shows a photodegradation mechanism similar to that of poly(vinyl chloride). The latter polymer has poor thermal and photochemical stability because of HCl elimination and the formation of conjugated polyenes.[2,3] Thus, it is necessary to use some additives to reduce the photodegradation of chlorinated resins. Normally, UV absorbers and quenchers are applied, most of which are organic compounds; this means that they are prone to transfer, volatilization, and degradation. This can lead to degradation and loss of function of the resin.

In recent years, nanometer-size materials have been widely studied in terms of their production, properties, and applications.[4–6] Nanometer-size TiO_2 can dramatically increase the strain to failure and scratch resistance of epoxy composites in comparison with micrometer-size TiO_2.[7] It has also been shown that rutile nanometer-size TiO_2 is an excellent UV protector that does not suffer from volatilization or degradation.[8–10] Thus, we studied the effect of nano-TiO_2 on the most widely used resin, MP-25. Because MP-25 is mainly used in anticorrosion coatings, saline immersion tests and UV weathering were conducted. Electrochemical impedance is a useful technique for evaluating the corrosion protection of coatings,[11–14] so this was also used for coating assessment. To evaluate the weathering of coatings and analyze the distribution of TiO_2 within the films, gloss measurements and X-ray photoelectron spectroscopy (XPS) were carried out.

EXPERIMENTAL

MP-25 resin (vinyl chloride–isobutyl vinyl ether copolymer; BASF) was dissolved in xylene with stirring at 1500 rpm for approximately 15 min.

Nanometer-size TiO_2 powder (P-25; average diameter = 21 nm), composed of 80% anatase and 20% rutile (Dusseldorf, Germany), and micrometer-size TiO_2 (R-930; average diameter = 0.2–0.4 μm; ISK, Osaka, Japan) were dispersed into xylene with the additive EFKA-4010 (EFKA, Basel, Switzerland) with stirring at 3000 rpm for a few minutes to produce a TiO_2 paste. Nanometer-size, pinlike TiO_2 (RM301 LP; average size = 50 nm × 10 nm; Duisburg, Germany) was also used to prepare a paste. Figure 1 shows transmission electron microscopy (TEM) images of P-25 and RM301 LP taken under a JEM-2000EX (Tokyo, Japan) microscope.

MP-25 was added to 5% TiO_2 paste and stirred to produce the following paints: S_1 with P-25, S_2 with R-930, and S_3 with RM301 LP.

Cold-rolled steel plates of 70 mm × 150 mm × 1 mm were used as the metal substrates for coating. The surface of the plates was pretreated by degreasing, polishing, washing, and drying before coating. Paints were coated onto the plates with an air spray to a desired dried film thickness of approximately 20 μm. The coated samples were allowed to cure at room temperature for a period of 1 week.
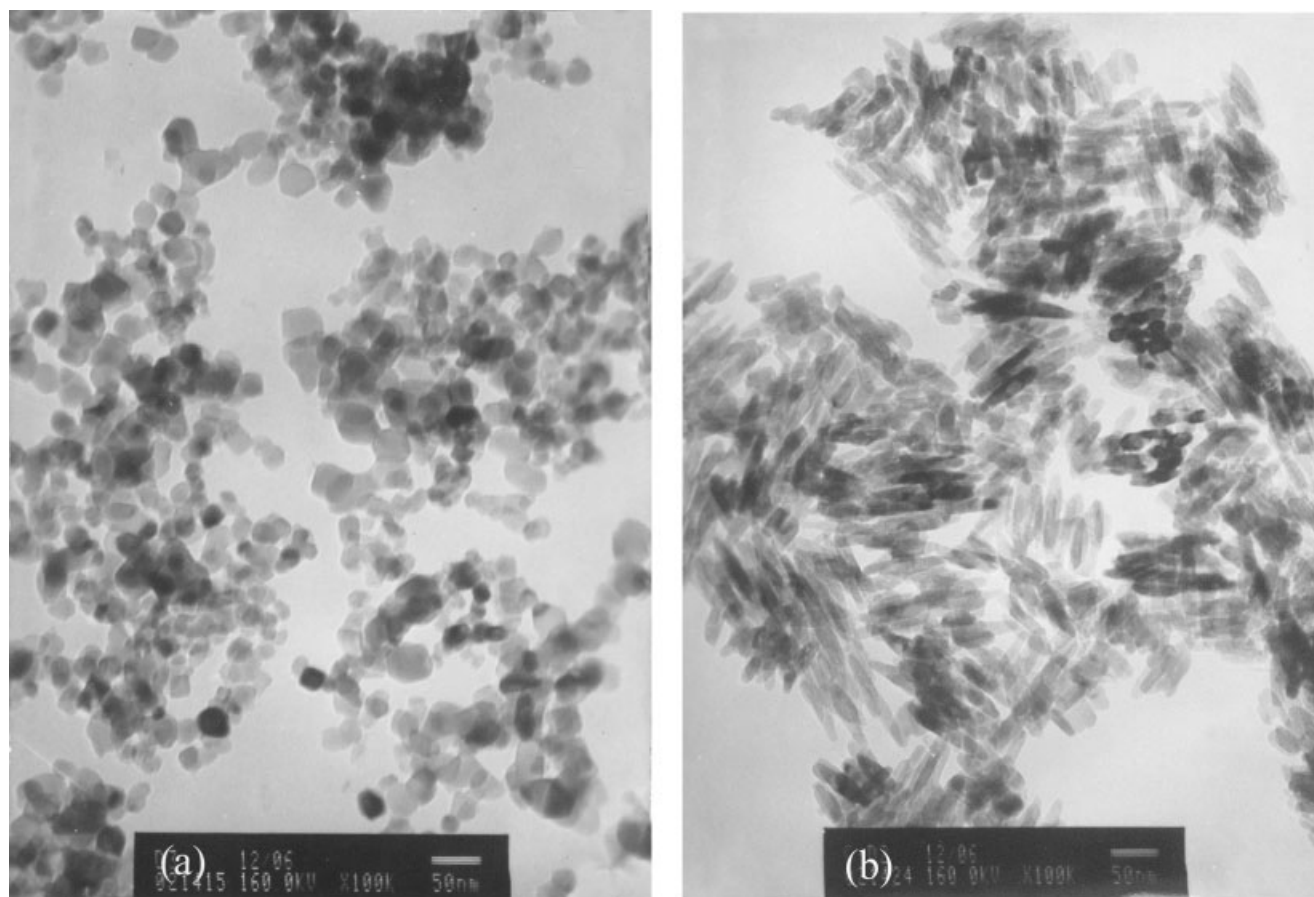

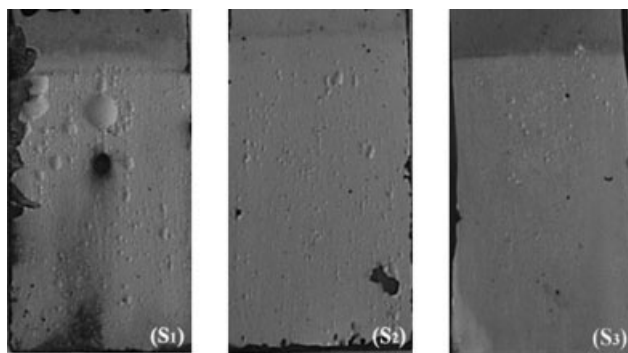**Figure 1** TEM images of (a) P-25 nano-TiO_2 and (b) RM301 LP.

Figure 2 Samples immersed in 40°C saline for 18 days.

The edges and backs of the specimens for immersion were sealed with a rosin–paraffin wax melt. To measure the electrochemical impedance, coated steel specimens were cut to a smaller size of 50 mm × 50 mm × 1 mm.

To minimize errors, three panels were immersed for each sample. The samples were immersed in 40°C saline water for 18 days and visually observed periodically. The results are shown in Figure 2.

Samples were photodegraded for 200 h in air at room temperature with germicidal UV lamps providing an intensity on the samples of 3.51 mW/cm^2 at 254 nm and 3 mW/cm^2 at 365 nm. Before and after UV exposure, gloss was measured at an incident angle of 60° with a KGZ-1B glossmeter (Tianjin, China).

XPS was used to investigate the surface composition of the coatings. Samples of 1 cm × 1 cm were cut from the panels for XPS tests with an Escalab MK-II (VG) instrument (Sussex, England). All samples were examined with Mg Kα radiation. The pressure in the analysis chamber during sample analysis was 10^{-13} Pa. To avoid affecting the carbon signal of coating components, carbon was scanned first, and this was followed by a general survey of the sample and then the rest of the elements (O, Cl, and Ti). Then, Ar$^+$ ion bombardment was used to remove the 100-nm outermost layer of the coating at 130 Å/min to investigate UV-induced damage to the MP-25 resin and the effect of TiO$_2$ on UV protection. Another general scan was then carried out. All C 1s peaks corresponding to hydrocarbons were calibrated at a binding energy of 285.0 eV to correct for the energy shift caused by charging. The area under each element peak was calculated, and the surface composition as an atomic percentage was then calculated with the elemental relative cross-sectional area as supplied by the XPS manufacturer. Curve fitting was carried out with XPSpeak4.1 (R. Kwok, Hongkong, China).

The electrochemical impedance investigation was conducted in a three-electrode system with a model 1287 lock-in amplifier interfaced to a Solartron 1260 potentiostat/galvanostat (Solartron, Hampshire, United Kingdom). The coated panel comprised a working electrode, platinum serving as a counter electrode, and a saturated calomel electrode as a reference electrode. The area exposed for examination was restricted with a plastic O-ring to 3.14 cm^2. The electrolyte was a 3% NaCl solution. Impedance data were automatically acquired with Zplot software (Solartron). A 10-mV alternating-current sine signal was applied to the electrode under potentiostat control in the frequency range of 0.01 Hz to 100 kHz. The impedance data were converted into Boukamp data format and then fitted to appropriate equivalent circuits with ZView analysis software.

RESULTS AND DISCUSSION

Saline immersion

After 18 days of immersion, all specimens were photographed (Fig. 2) and visually observed. Panels of S$_2$ and especially S$_1$ were corroded, with large blisters and rust spots, whereas S$_3$ panels showed only some small blisters, without obvious corrosion.

The results indicate that S$_1$ samples with P-25 did not endure saline immersion well, and S$_2$ samples with R-930 could bear saline immersion to some extent, but S$_3$ samples with RM301 LP showed excellent saline immersion resistance. This difference might be attributed to the different surface treatment methods and particle sizes of TiO$_2$. Other research has shown that the surface of P-25 is hydrophilic, whereas that of RM301 LP is hydrophobic.[15] Hence, these compounds react differently to saline immersion, despite having almost the same particle size. R-930 is a pigmental white powder with a particle size of 200–400 nm, which is much larger than that of RM301 LP, so their filling abilities in coatings are distinctly different. A pigment (especially its particle size, morphology, and surface state) has a significant effect on the penetration of water and oxygen into a coating film. Dehri and Erbil[16] showed that the polymer has inherent pores with a diameter of 1–100 nm, which represent the main path for corrosive materials, so nano-TiO$_2$ could fill many more holes in the resin and prevent the penetration of water and oxygen more easily.

Gloss changes

Sample gloss was measured before and after exposure to UV light for 200 h. The results are listed in Table I.

The initial gloss of the three sample types was the same, and this indicates that the MP-25 resin had high gloss. After 200 h of UV exposure, the gloss of samples with RM301 LP showed the least change, whereas the gloss of samples with P-25 and R-930

TABLE I
Gloss Change for the Samples Before and After 200 h of UV Exposure

Sample	Before exposure	After 200 h of exposure	Change ratio (%)
S$_1$	95.2	1.8	98.1
S$_2$	95.2	2.8	97.1
S$_3$	95.2	62.6	34.2

changed dramatically. Gloss change is a function of the roughness of the coating surface, which indicates degradation of the polymer coating and aggregation of pigment particles on the surface. The greater the gloss change is, the greater the degradation is of the coating polymer. P-25 is a mixture of 80% anatase and 20% rutile that shows great catalytic ability because of its mixed crystalline structure, so it is not surprising that sample S$_1$ with P-25 was highly degraded. The results show that RM301 LP has excellent UV-screening ability compared to P-25 and R-930 for MP-25, although R-930 is a well-known UV-screening agent. The results for gloss measurement are consistent with the XPS analysis. Therefore, RM301 LP could represent a good UV-resistant additive.

XPS analysis

To compare UV aging of the coatings, samples S$_1$, S$_2$, and S$_3$ with and without UV exposure were analyzed by XPS. General scans of S$_1$, S$_2$, and S$_3$ samples were carried out. The stoichiometric ratios of C, O, Cl, and Ti in the samples before and after Ar$^+$ ion sputtering are listed in Table II. C and Cl originate from the MP-25 resin, and Ti comes from added TiO$_2$, whereas O belongs to TiO$_2$ and MP-25. In the surface (outermost) layer (before Ar$^+$ ion sputtering), chlorine decreased whereas oxygen and titanium increased for UV-exposed samples in comparison

TABLE II
Stoichiometric Ratios of C, O, Cl, and Ti in the Samples Before and After Ion Sputtering

Sample	Stoichiometric ratio			
	C 1s	O 1s	Cl 2p	Ti 2p
S$_1$ (UV)	1.000	1.788	0.065	0.254
S$_1$ (UV + IE)	1.000	7.165	0.651	1.698
S$_1$	1.000	0.202	0.148	0.006
S$_1$ (IE)	1.000	0.024	0.029	0.009
S$_2$ (UV)	1.000	0.608	0.043	0.010
S$_2$ (UV + IE)	1.000	0.333	0.088	0.112
S$_2$	1.000	0.191	0.159	0.004
S$_2$ (IE)	1.000	0.018	0.026	0.005
S$_3$ (UV)	1.000	0.501	0.085	0.017
S$_3$ (UV + IE)	1.000	0.321	0.145	0.193
S$_3$	1.000	0.202	0.154	0.004
S$_3$ (IE)	1.000	0.064	0.026	0.032

IE, samples after ion sputtering.

with those without UV exposure. This indicates that UV exposure accelerated the dechlorination of MP-25 resin. A comparison of the outermost layer with the inner layer (after Ar$^+$ ion sputtering) of UV-exposed samples shows that oxygen was higher, except for S$_1$, whereas chlorine and titanium were lower. However, for samples without UV exposure, oxygen and chlorine were higher and titanium was lower in the outermost layer. Therefore, it can be inferred that oxygen and chlorine tended to distribute in the outermost layer, the so-called skin effect of oxygen and chlorine, whereas titanium tended to distribute in the inner layer. Moreover, bonds between carbon and chlorine tended to break under UV exposure. Consolati et al.[17] used γ radiation to study polyurethane aircraft skin coatings with TiO$_2$ and found that there was a resin layer about 10 nm thick and then a 1-μm layer with much TiO$_2$; this is consistent with the XPS results in this study. The reason for this might be the large size of TiO$_2$ particles, which were wrapped by the resin under surface tensile strength. As for the exception of oxygen distribution in S$_1$, it might be due to the much greater degradation of carbon chains in MP-25 resin, such as oxidization and dechlorination, which resulted in the carbon content decreasing greatly (Fig. 3) and oxygen ratio increasing in the carbon chain. Because small and volatile oxygen-containing materials, such as carbon monoxide, occurred in the outermost layer, oxygen in the inner layer was higher than that in the outermost layer.

Figure 3 compares C 1s spectra of samples before and after UV aging. The results show that the carbon content of samples after UV exposure was greatly decreased, and a bonding energy peak at more than 288 eV appeared, which can be attributed to carboxyl or other groups. This indicates that the resin
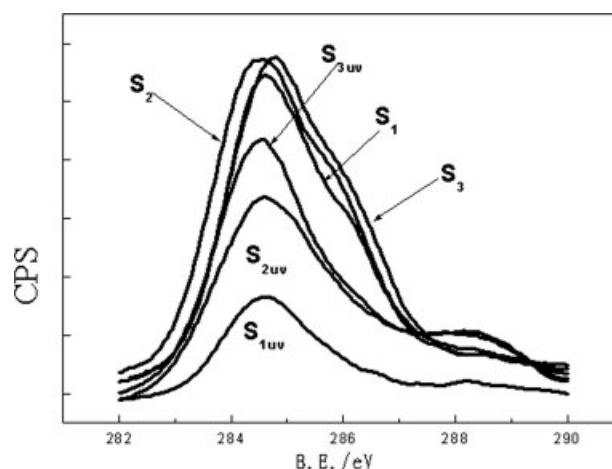

Figure 3 C 1s XPS spectra of the coating samples before and after UV aging. S$_{1uv}$ is sample S$_1$ after 200 h of UV exposure; B.E. is the bonding energy. CPS, counter per second, a kind of relative intensity unit.
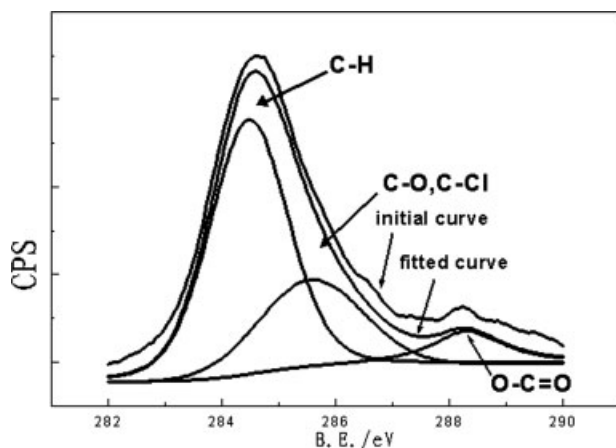
Figure 4 XPS fitting curve for C 1s of S_1 after UV aging. B.E. is the bonding energy.

likely degraded because of carbon chain breakage and the release of volatile materials, such as carbon dioxide, due to photocatalytic aging.

Figure 4 shows three fitted peaks at bonding energies of 284.5, 285.7, and 288.3 eV. According to the literature, these can be attributed to C 1s of C—H, C—O and C—Cl, and O=C—O, respectively.[18] In comparison with the samples without UV exposure shown in Figure 5, there was a shift of 0.5 eV in the bonding energy from 286.2 to 285.7 eV. This might be due to a group or atom bonded to carbon with lower electronegativity, and thus the negative charge density of carbon increased. The bonding energy is lower for C—O than for C—Cl groups, and the electronegativity of O is lower than that of Cl. Therefore, the shift can be attributed to the breakage of C—Cl bonds, which resulted in a decrease in C—Cl and an increase in C—O, confirming the dechlorination of MP-25 after UV exposure.
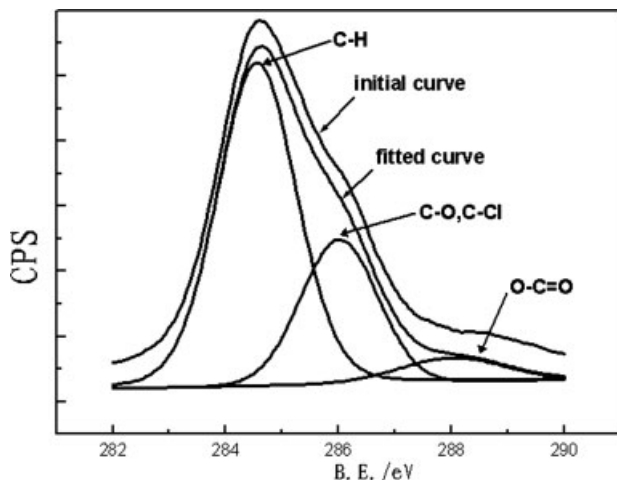

Figure 5 XPS fitting curve for C 1s of the S_1 surface before UV aging. B.E. is the bonding energy.
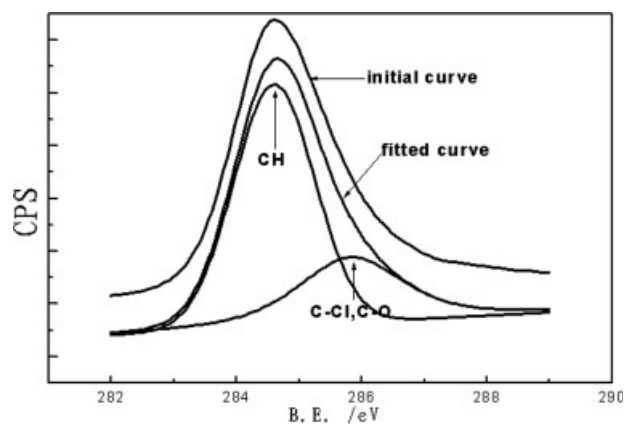
Figure 6 XPS fitting curve for C 1s of the inner layer of S_1 before UV aging. B.E. is the bonding energy.

Figures 5 and 6 show that O—C=O was present in the outermost layer, and this is consistent with the Fourier transform infrared (FTIR) peak near 1730 cm^{-1} previously identified,[15] although UV exposure was not used. However, in the inner layer, O—C=O was almost absent. Table III shows that the O—C=O content in the outermost layer of UV-exposed samples was different for the three types of TiO$_2$: S_1 with P-25 had the lowest content, whereas S_3 with RM301 LP had the highest. According to FTIR, O—C=O groups are mainly present in antiaging additives in the MP-25 resin. Hence, a higher O—C=O content of samples after UV exposure represents better UV shielding by the added TiO$_2$.

Electrochemical impedance

The behavior of panels was followed by impedance measurements for the whole immersion period. Because impedance in the low-frequency region reflects the coating barrier property, which in turn reflects the anticorrosion integrity of the coating,[19]

TABLE III
C 1s Components in the Experimental Samples

Sample	Area of C 1s peak (%)		
	C—H	C—O, C—Cl	O—C=O
S_1 (UV)	72.24	28.74	0.02
S_1 (UV + IE)	72.90	27.10	0.00
S_1	63.90	25.99	10.11
S_1 (IE)	66.66	33.34	0.00
S_2 (UV)	63.08	36.56	0.36
S_2 (UV + IE)	60.96	39.04	0.00
S_2	57.42	22.70	19.88
S_2 (IE)	83.42	16.58	0.00
S_3 (UV)	65.88	29.49	4.63
S_3 (UV + IE)	68.91	31.09	0.00
S_3	61.86	21.71	16.33
S_3 (IE)	72.86	27.14	0.00

IE, samples after ion sputtering.

TABLE IV
Impedance (Ω cm^2) of the Three Sample Types at 0.07455 Hz for Different Immersion Times

Time	S$_1$	S$_2$	S$_3$
5 h	62,778	27,8410	44,4390
1 day	37,851	10,1460	30,1520
2 days	34,161	76,546	23,9480
4 days	11,619	46,835	27,2930
8 days	5,031.4	21,687	183,290

we focused on the values of the impedance modulus at 0.07455 Hz ($|Z|_{0.07455\ Hz}$) after exposure for different time intervals. Generally, coatings that exhibit higher $|Z|_{0.07455\ Hz}$ also display better corrosion protection. Examples of the evolution of $|Z|_{0.07455\ Hz}$ with the exposure time are presented in Table IV. In general, the impedance modulus decreased with the exposure time, and this showed a loss of protective properties of the coatings.

The impedance of S$_1$ samples rapidly decreased with the immersion time, and large blisters (diameter $\sim$ 2 mm) and rust were observed on the panels at the end of the immersion test. The impedance of S$_2$ samples decreased more slowly with time than that of S$_1$. The impedance of S$_3$ samples also decreased with time, but only slightly. Thus, an evaluation of the anticorrosion properties based on impedance showed that samples with rutile nano-TiO$_2$ RM301 LP were the best, whereas those with P-25 were the worst. The reason for this might be the hydrophilic surface property, as discussed previously. The difference in impedance for the same weight of nanosized and ordinary TiO$_2$ might be attributed to the equivalent pigment volume concentration. Nano-TiO$_2$ has a much larger specific surface area and specific volume, so it can contact more resin molecules and fill more holes within and between resin molecules, thus showing a greater barrier capacity against aggressive materials such as water and electrolytes. Therefore, it can be inferred that the amount of pigment required would be much smaller for nanosized materials to achieve the same critical pigment volume concentration (CPVC).

CONCLUSIONS

The addition of rutile nano-TiO$_2$ RM301 LP to MP-25 resin can improve its immersion resistance, weathering resistance, and anticorrosion properties. The addition of P-25 accelerates the aging of MP-25 in comparison with R-930, a good UV-screening additive for polymers.

MP-25 resin degrades under UV irradiation via dechlorination and C—C bond breakage, similarly to poly(vinyl chloride), but the addition of nano-TiO$_2$ RM301 LP can delay the degradation of MP-25.

Rutile nano-TiO$_2$ RM301 LP drastically decreases the requirement for pigment addition to achieve CPVC for coating formulas and can be used in coatings based on MP-25 resin.

Chlorine and oxygen in MP-25 have a skin effect.

References

1. Hu, A.; Zhang, X. China Paint 2005, 20, 37.
2. Gardette, J. L.; Lemaire, J. Polym Degrad Stab 1991, 34, 135.
3. Torikai, A.; Hasegawa, H. Polym Degrad Stab 1999, 63, 441.
4. Yang, S.; Liu, Y.; Guo, Y.; Zhao, J.; Xu, H.; Wang, Z. Mater Chem Phys 2002, 77, 501.
5. Zhang, R.; Gao, L. Mater Res Bull 2001, 36, 1957.
6. Colón, G.; Hidalgo, M. C.; Navío, J. A. Catal Today 2002, 76, 91.
7. Ng, C. B.; Schadler, L. S.; Siegel, R. W. Nanostruct Mater 1999, 12, 507.
8. Allen, N. S.; Edge, M.; Ortega, A. Liauw, C.; Stratton, J.; McIntyre, R. Polym Degrad Stab 2002, 78, 467.
9. Turton, T. J.; White, J. R. Polym Degrad Stab 2001, 74, 559.
10. Gesenhues, U. Polym Degrad Stab 2000, 68, 185.
11. Kending, M.; Mansfeld, F.; Tsai, S. Corros Sci 1983, 23, 317.
12. Mansfeld, F.; Lee, C. C.; Zhang, G. Electrochim Acta 1998, 43, 435.
13. McQueen, R. C.; Granata, R. D. Prog Org Coat 1996, 28, 97.
14. McCluney, S. A.; Popova, S. N.; Popov, B. N.; et al. J Electrochem Soc 1992, 139, 1556.
15. Bin, X. Ph.D. Dissertation, Chinese Academy of Science, Beijing, China, 2004.
16. Dehri, I.; Erbil, M. Corros Sci 2000, 42, 969.
17. Consolati, G.; Levi, M.; Turri, S. Polymer 2001, 42, 9723.
18. Briggs, D. Surface Analysis of Polymers by XPS and Static SIMS; Cambridge University Press: Cambridge, UK, 1998; p 67.
19. Yang, X. F.; Li, J.; Croll, S. G.; Tallman, D. E.; Bierwagen, G. P. Polym Degrad Stab 2003, 80, 56.